PAS-LuxR transcriptional control of filipin biosynthesis in *S. avermitilis*

**Cláudia M. Vicente · Javier Santos-Aberturas ·
Tamara D. Payero · Eva G. Barreales ·
Antonio de Pedro · Jesús F. Aparicio**

Abstract The DNA region encoding the filipin gene cluster in *Streptomyces avermitilis* (*pte*) contains a PAS-LuxR regulatory gene, *pteF*, orthologue to *pimM*, the final pathway-specific positive regulatory protein of pimaricin biosynthesis in *Streptomyces natalensis*. Gene replacement of the gene from *S. avermitilis* chromosome resulted in a severe loss of filipin production and delayed spore formation in comparison to that of the wild-type strain, suggesting that it acts as a positive regulator of filipin biosynthesis and that it may also have a role in sporulation. Complementation of the mutant with a single copy of the gene integrated into the chromosome restored wild-type phenotypes. Heterologous complementation with the regulatory counterpart from *S. natalensis* also restored parental phenotypes. Gene expression analyses in *S. avermitilis* wild-type and the mutant by reverse transcription-quantitative polymerase chain reaction of the filipin gene cluster suggested the targets for the regulatory protein. Transcription start points of all the genes of the cluster were studied by 5′-rapid amplification of complementary DNA ends. Transcription start point analysis of the *pteF* gene revealed that the annotated sequence in the databases is incorrect. Confirmation of target promoters was performed by in silico search of binding sites among identified promoters and the binding of the orthologous regulator for pimaricin biosynthesis PimM to gene promoters by electrophoretic mobility shift assays. Precise binding regions were investigated by DNAse I protection studies. Our results indicate that PteF activates the transcription from two promoters of polyketide synthase genes directly, and indirectly of other genes of the cluster.

C. M. Vicente · J. Santos-Aberturas · T. D. Payero · E. G. Barreales · A. de Pedro · J. F. Aparicio (✉)
Area de Microbiología, Facultad de Biología, Universidad de León, Campus de Vegazana s/n, 24071 León, Spain
e-mail: chusaparicio33@gmail.com

C. M. Vicente · J. Santos-Aberturas
Instituto de Biotecnología INBIOTEC, Avda. Real, n° 1, 24006 León, Spain

Present Address:
J. Santos-Aberturas
Institute of Biochemistry, Department of Biotechnology and Enzyme Catalysis, University of Greifswald, Felix-Hausdorff-Str. 4, 17487 Greifswald, Germany

Introduction

Streptomyces are soil-dwelling filamentous bacteria well-known for their ability to produce a variety of antibiotics and other secondary metabolites. Production of these compounds is regulated in response to nutritional status alteration, population density and a variety of environmental conditions and hence occurs in a growth-phase-dependent manner and usually accompanied by morphological differentiation (Martín et al. 2000; Bibb 2005; Liu et al. 2013).

Filipin is a 28-membered ring pentaene macrolide antifungal antibiotic produced by *Streptomyces filipinensis*, *Streptomyces avermitilis* and other *Streptomyces* strains (Whitfield et al. 1955; Ikeda et al. 2014; Kim et al. 2012). It represents the archetype of non-glycosylated polyenes, and as a polyene, it interacts with membrane sterols, thus causing the alteration of membrane structure and leading to the leakage of cellular materials (Aparicio et al. 2004). Contrary to most polyene macrolides which display higher affinity for ergosterol (the main sterol in fungal membranes) than for other sterols, filipin shows a similar affinity for cholesterol and ergosterol.

This property makes it useless for its application in human therapy due to its toxic side effects but has permitted its application as a tool for the diagnosis of Niemann-Pick type C disease, a characteristic cholesterol overloaded lysosomal disorder of genetic origin (Kruth et al. 1986), and as a probe for the detection and quantification of cholesterol in cellular membranes (Gimpl and Gehrig-Burger 2011). As other macrocyclic polyketides, filipin is synthesized by the action of type I modular polyketide synthases. Its biosynthetic gene cluster (*pte*) has been identified in the avermectin-producing *S. avermitilis* NRRL 8165 upon sequencing of its genome and encodes 14 polyketide synthase modules within five multifunctional enzymes and eight additional proteins that presumably govern modification of the polyketide skeleton and regulation of gene expression (Fig. 1a) (Omura et al. 2001; Ikeda et al. 2003). In nature, filipin is produced as a mixture of related compounds known as the filipin complex (filipins I to IV) (Fig. 1b) (Bergy and Eble 1968), being filipin III the major component.

Control of secondary metabolite production is a complex process involving multiple signals and an intricate network of regulators that cross-talk with each other (Martín and Liras 2010). Generally, the lowest level of this network is played by regulatory genes that only affect a single antibiotic biosynthetic pathway. These pathway-specific regulatory genes are usually found within the respective antibiotic biosynthesis gene cluster. Two distinct regulators of filipin biosynthesis are encoded by genes located in the *pte* cluster, *pteR* and *pteF* (Ikeda et al. 2003).

PteR is orthologous to the transcriptional activator of pimaricin biosynthesis PimR, an archetype of a particular class of regulators that combine an N-terminal DNA-binding domain corresponding to the SARP family of transcriptional activators with a C-terminal half homologous to guanylate

cyclases and large ATP-binding regulators of the LuxR family (LAL) (Antón et al. 2004). The C-terminal half includes the ATP/GTP-binding domain characteristic of these protein families but lacks the characteristic signature sequence at the N-terminus of guanylate cyclases or the LuxR-type helix-turn-helix (HTH) motif for DNA binding present at the C-terminus of LAL regulators. Members of this class also include the nikkomycin activator in *Streptomyces ansochromogenes* SanG (Liu et al. 2005) or the polyoxin regulator in *Streptomyces cacaoi* PolR (Li et al. 2009). Recently, we have characterized the PimR mode of action and determined that it binds an operator that contains three heptameric direct repeats of the consensus CGGCAAG with 4 bp spacers (Santos-Aberturas et al. 2012).

In turn, PteF is orthologous to PimM, the second activator of pimaricin biosynthesis (Antón et al. 2007). These PAS/LuxR regulators combine an N-terminal PAS sensory domain with a C-terminal HTH motif of the LuxR type. Recently, we have carried out the molecular characterization of PimM mode of action and determined the canonical binding site of this regulator as CTVGGGAWWTCCCBAG, just at the -35 hexamer of regulated promoters in *Streptomyces natalensis* (Santos-Aberturas et al. 2011b). Noteworthy, PimM homologous regulatory proteins have been found to be encoded in all known biosynthetic gene clusters of polyene polyketides (Santos-Aberturas et al. 2011b). PimR and PimM act in a hierarchical way, PimR binds *pimM* promoter and activates its transcription (Santos-Aberturas et al. 2012), and the gene product of the latter activates transcription from eight different promoters of pimaricin structural genes directly (Santos-Aberturas et al. 2011a).

In order to understand if there is a molecular mechanism of polyene control common to all actinomycetes, it was of great interest to study the transcriptional control of the filipin genes

Fig. 1 Organizations of the filipin biosynthetic gene cluster and structure of filipins. **a** The *pointed boxes* indicate the direction of transcription. The *pteF* gene is indicated in *black* and the polyketide synthase genes are shown as *stripped pointed boxes*. The *arrows* indicate deduced transcriptional units. *Square boxes* are DNA fragments used in mobility shift experiments (sizes (bp) are indicated below). **b** Filipin I: R_1=H, R_2=H; filipin II: R_1=OH, R_2=H; filipin III: R_1= OH, R_2=OH. Filipin IV is a stereoisomer of filipin III
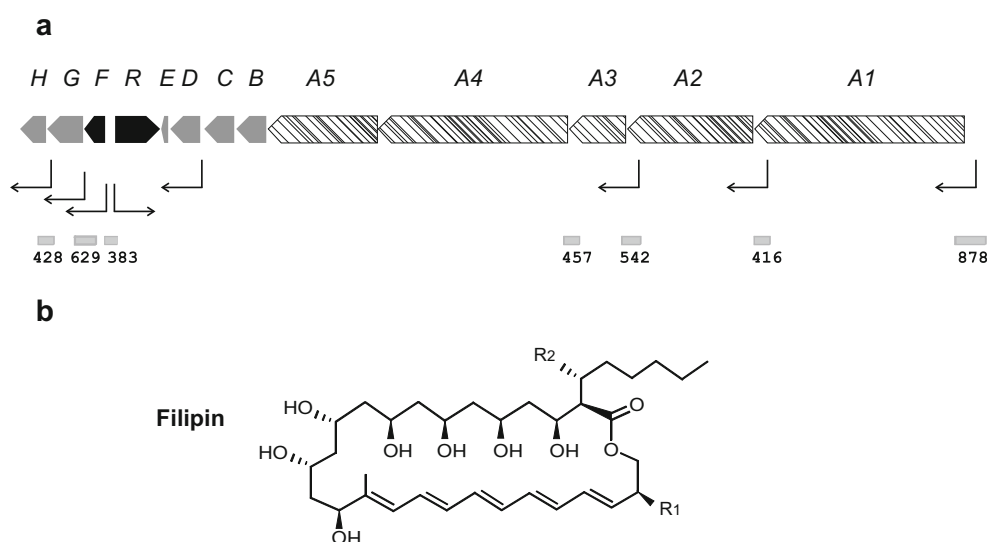
(*pte*) of *S. avermitilis* by the pathway-specific regulator PteF. In this work, we have generated mutants of the regulator and characterized its mode of action.

Materials and methods

Bacterial strains and cultivation

S. avermitilis NRRL 8165 was routinely grown in yeast extract-malt extract (YEME) medium (Kieser et al. 2000) without sucrose. Sporulation was generally achieved in TBO medium (Higgens et al. 1974) at 30 °C. Spore production was assessed in YEME, TBO and minimal medium (Kieser et al. 2000) by spreading 2.5×10^6 spores of the mutant and the parental strain and incubation at 30 °C for 5, 7 and 10 days. After making the spore suspension, spore counting was done by plating serially diluted spore suspension on TSA medium. *Escherichia coli* strain DH5α was used as a host for DNA manipulation. *E. coli* BL21 (DE3) was used for expression studies. *E. coli* BW25113 [pIJ790] was used for gene replacement experiments. *E. coli* ET12567 [pUZ8002] was used as donor in intergeneric conjugations. *Candida utilis* (syn. *Pichia jadinii*) CECT 1061 was used for bioassay experiments.

Plasmids and DNA manipulation procedures

Standard genetic techniques with *E. coli* and in vitro DNA manipulations were as described by Sambrook and Russell (2001). Recombinant DNA techniques in *Streptomyces* species and isolation of *Streptomyces* total DNA were performed as previously described (Kieser et al. 2000). Southern hybridization was carried out with probes labelled with digoxigenin by using the DIG DNA labelling kit (Roche Biochemicals). Intergeneric conjugation between *E. coli* ET12567 [pUZ8002] and *S. avermitilis* was performed as described (Enríquez et al. 2006). pUC19 (New England Biolabs) was used as the routine cloning vector, pSETneo (Am^R, Kan^R, pUC18 replicon, ΦC31 *attP*; Vicente et al. 2009) was used for intergeneric conjugation and pJM^DBD was the vector used for protein expression (Santos-Aberturas et al. 2011a). Polymerase chain reactions were carried out using Phusion DNA Polymerase as described by the enzyme supplier (Finnzymes). DNA sequencing was accomplished by the dideoxynucleotide chain-termination method using the Perkin Elmer Amplitaq Gold Big Dye-terminator sequencing system with an Applied Biosystems ABI 3130 DNA genetic analyzer (Foster City, CA, USA).

Construction of ΔpteF mutant

Deletion of *pteF* from *S. avermitilis* chromosome was made by replacing the wild-type gene with a cassette containing an apramycin selective marker using a PCR-based system (Gust et al. 2003). The plasmid pIJ773 containing the apramycin resistance gene (*aac(3)IV*) and the *oriT* replication origin was used as a template. The mutant was constructed using the oligonucleotides 5′-*ccgcgcgagcgggcgccgggagggcccgatgcccgctca*TGTAGG CTGGAGCTGCTTC-3′ and 5′-*gttcaacatctggcgataccgctggtcccagggccgatg*ATTCCGGGGATC CGTCGACC-3′ as the forward and reverse primers, respectively (the sequence identical to the DNA segment upstream from the start codon of *pteF* is in lower case italics and the sequence identical to the segment downstream from the stop codon of *pteF* is underlined and in lower case). These two long PCR primers (59 and 58 nt) were designed to produce a deletion of *pteF* just after its start codon, leaving only its stop codon behind. The 3′ sequence of each primer matches the right or left end of the disruption cassette (the sequence is shown uppercase in both primers). The extended resistance cassette was amplified by PCR, and *E. coli* BW25113 [pIJ790] bearing cosmid CL240_D05 was electro-transformed with this cassette. The isolated mutant cosmid was introduced into non-methylating *E. coli* ET12567 containing the RP4 derivative pUZ8002. The mutant cosmid was then transferred to *S. avermitilis* by intergeneric conjugation. Double cross-over exconjugants were screened for their apramycin resistance followed by confirmation by both PCR and Southern blot analysis (Fig. S1).

Construction of plasmids for gene complementation

In order to complement *pteF* replacement mutant, a 1,122-bp DNA fragment containing the entire *pteF* gene plus its own promoter was amplified by PCR with primers pteF fw (5′-GAGGTGCTTCTCCCGTG-3′) and pteF rev (5′-CCATCG TGCTTGCGG-3′) using *S. avermitilis* chromosomal DNA as template. The PCR product was ligated into a EcoRV-cut pSETneo to yield pSETneo::pteF.

For the heterologous complementation of *S. avermitilis* Δ*pteF*, the entire *pimM* gene plus its own promoter region were amplified by PCR using the primers pimM+P forward (5′-GGTTGAATTCTTGCGGTCGGTGGTGCGGGC-3′) and pimM+P reverse (5′-GTCGTCCTCGGGTTCTTGCGG-3′) using *S. natalensis* chromosomal DNA as template. The PCR product was ligated into a EcoRV-digested pSETneo to obtain pSETneo::pimM.

Isolation of total RNA

For RNA extraction, 2 ml from liquid cultures in YEME medium without sucrose was harvested by centrifugation and immediately frozen by immersion in liquid nitrogen. Cells were resuspended in lysis solution [600 μl RLT buffer (RNeasy Mini Kit; Qiagen); 60 μl 2-mercaptoethanol] and disrupted using a sonicator (Ultrasonic processor XL; Misonix Inc.). RNeasy ® Mini kit (Qiagen) was used for RNA isolation using RNase-

Free DNase Set (Qiagen) as specified by the manufacturer, followed by two consecutive digestions with TURBO[TM] DNase from Ambion® according to the manufacturer's instructions.

Reverse transcriptase-PCR experiments

Transcription was studied by using the SuperScript[TM] One-Step reverse transcriptase-PCR (RT-PCR) system with Platinum® Taq DNA polymerase (Invitrogen), using 150 ng of total RNA as template. Conditions were as follows: first strand complementary DNA (cDNA) synthesis, 45 °C for 40 min followed by heating at 94 °C for 2 min; amplification, 30 cycles of 94 °C for 40 s, 63–67 °C (depending of the set of primers used) for 30 s, and 72 °C for 1 min. Primers (18–26 mers; Table S1) were designed to cover intergenic regions, generating PCR products of approximately 300–800 bp. Negative controls were carried out with each set of primers and Platinum® Taq DNA polymerase in order to confirm the absence of contaminating DNA in the RNA preparations. The identity of each amplified product was corroborated by direct sequencing of the PCR product.

Rapid amplification of cDNA ends

The 5′ ends of transcripts were identified by using a 5′ rapid amplification of cDNA ends (RACE) system for rapid amplification of cDNA ends kit (Invitrogen) following the manufacturer's instructions (version 2.0). Briefly, first strand cDNA synthesis was carried out using 5 μg of total RNA, reverse transcriptase and the gene-specific primer (numbers 1 in Table S2). The cDNA was purified using the SNAP columns provided in the kit, and poly (dC) tails were added to the 3′ ends using terminal deoxynucleotidyl transferase. PCR amplification of the tailed cDNA was carried out using the 5′ RACE abridged anchor primer with the first nested primer (numbers 2 in Table S2). A dilution of the PCR mixture was then subjected to reamplification using the abridged universal amplification primer with the second nested primer (numbers 3 in Table S2). The PCR products were gel-purified and sequenced. When cDNA tailing with poly(dC) did not permit the identification of the transcription start point, poly(dA) tails were added to the 3′ ends of cDNA. In these cases, second strand cDNA synthesis was necessary prior to nested amplifications and was carried out using the 3′ RACE adapter primer (Invitrogen). PCR amplification of the cDNA was then carried out using the abridged universal amplification primer with the first nested primer (numbers 2 in Table S2). Final nested amplification was carried out as before.

Reverse transcription-quantitative PCR

Reverse transcription of total RNA was performed on selected samples with 5 μg of total RNA and 12.5 ng/μl of random hexamer primer (Invitrogen) using SuperScript™ III reverse transcriptase (Invitrogen) according to the manufacturer's instructions. All RNA samples were analyzed with the Agilent 2100 bioanalyzer (Agilent Technologies, Palo Alto, CA) and only those with RNA integrity number (RIN) values (Schroeder et al. 2006) raging from 8.0 to 9.0 were selected. Each reaction was performed in 20 μl with SYBR® Premix Ex Taq[TM] (TaKaRa), and 100–350 nM of each primer and the template cDNA 1:2 diluted and run on a StepOnePlus Real-Time PCR system (Applied Biosystems). Reactions were carried out on three biological replicates with three technical replicates each and appropriate controls were included to verify the absence of gDNA contamination in RNA and primer-dimer formation. Primers (see Table S3) were designed to generate PCR products between 96 and 153 bp, near the 5′-end of messenger RNA (mRNA) using the Primer3 software (Rozen and Skaletsky 2000). The PCR reactions were initiated by incubating the sample at 95 °C for 10 min followed by 40 cycles at 95 °C for 15 s, 62–70 °C (depending of the set of primers used) for 34 s. To check the specificity of real-time PCR reactions, a DNA melting curve analysis was performed by holding the sample at 60 °C for 60 s followed by slow ramping of the temperature to 95 °C. SYBR fluorescence was normalized by ROX fluorescence. Baseline and threshold values were determined by the StepOnePlus software. C_t values were normalized with respect to $rrnA1$ mRNA (encoding 16S ribosomal RNA (rRNA)). Relative changes in gene expression were quantified using the Pfaffl (2001) method and the REST© software (Pfaffl et al. 2002). The corresponding real-time PCR efficiency (E) of one cycle in the exponential phase was calculated according to the equation $E=10^{[-1/\text{slope}]}$ (Rasmussen 2000) using fivefold dilutions of genomic DNA raging from 0.013 to 40 ng ($n=5$ or 6 with three replicates for each dilution) with a coefficient of determination $R^2>0.98$ (Fig. S2).

DNA-protein binding assays

DNA binding tests were performed by electrophoretic mobility shift assay (EMSA). The DNA fragments used for EMSA were amplified by PCR using the primers listed in Table S4, and either directly labelled at both ends with digoxigenin with DIG Oligonucleotide 3′-End Labeling Kit, 2nd Generation (Roche Applied Science) or first cloned into pUC19, and then amplified by PCR using the universal and reverse primers, one of them labelled with 6-carboxyfluorescein. Binding assays were performed with GST-PimM[DBD], protein as described previously (Santos-Aberturas et al. 2011b, 2012).

Footprinting assays

DNase I footprinting assays were performed by the fluorescent labelling procedure, using the GST-PimM^{DBD} protein as described in Santos-Aberturas et al. (2011a). The DNA fragment used was the same as that used for EMSA experiments labelled with 6-carboxyfluorecein as described above. In each case, the same unlabelled oligonucleotide served to prime the sequencing reaction. The PCR products were purified after agarose-gel electrophoresis and DNA concentrations were determined with a NanoDrop ND-1000 spectrophotometer (Thermo Scientific).

DNase I footprinting was performed by incubating 0.28 pmol of the DNA probe and GST-PimM^{DBD} protein for 10 min at 30 °C. Lyophilized bovine pancreas DNase I (Roche grade I) was reconstituted in 20 mM Tris-HCl pH 7.0, 50 mM NaCl, 100 μg/ml BSA, 1 mM DTT and 10 % glycerol to a final concentration of 2.5×10^{-3} units/μl. Nuclease digestions were carried out with 0.01 units (4 μl) at 30 °C for 1 min and stopped with 120 μl of 40 mM EDTA in 9 mM Tris-HCl pH 8.0. After phenol-chloroform purification and ethanol precipitation, samples were loaded in an Applied Biosystems ABI 3130 DNA genetic analyzer (Foster City, CA, USA). Results were analysed with the Peak Scanner program (Applied Biosystems).

Assay of filipin production

To assay filipin in culture broths, 8 ml of culture was extracted with 16 ml of ethyl acetate and the organic phase was vacuum-dried and resuspended in 200 μl of pure methanol. Solutions of pure filipin III (Sigma) were used as control. Quantitative determination of filipin III was assessed by reverse-phase high performance liquid chromatography (HPLC) using a Waters 600 unit coupled to a PDA 996 detector equipped with a Mediterranea Sea C18 column (4.6×150 mm, particle size 3 μm) (Teknokroma). Elution was performed with a gradient (0.8 ml/min) of methanol-0.1 % formic acid according to the following program: 50:50 v/v 0–3 min, up to 90:10 v/v 3–12 min, 90:10 12–20 min, up to 100:0 v/v 20–21 min, 100:0 v/v 21–23 min, down to 0:100 v/v 23–24 min, 0:100 v/v 24–26 min, up to 50:50 v/v 26–27 min, 50:50 v/v 27–32 min. Retention time for filipin III was 18.2 min. When required, the fungicidal activity of filipin was tested by bioassay using *C. utilis* CECT 1061 as test organism.

Bioinformatic analysis

Candidate sequences to contain promoters were analyzed using the Patser algorithm (Hertz and Stormo 1999), implemented in the web resource Regulatory Sequence Analysis Tools (van Helden 2003). The pseudocount value was set to 10, and the alphabet parameter was adjusted to the GC content of *Streptomyces* genome: AT, 0.15; CG, 0.35. The matrices used to search for regions -35 and -10 were those derived from the alignments of class C and class A promoters of Bourn and Babb (1995). To search for a combination of 'class C–n nucleotides of separation–class A', we included n columns of null values in the combined matrix. To calculate the information content (R_i value) of individual sequences (Schneider 1997) and to obtain the logo of the binding site of the regulator PimM, we used the BiPad Server (Bi and Rogan 2006).

Results

Organization of *pte* cluster transcriptional units

In order to define an overall picture of the transcriptional arrangement of the *pte* genes, an accurate identification of operons was needed. We thus decided to analyze the possible co-transcription of neighbouring genes by reverse transcriptase-polymerase chain reaction experiments. Total RNA was prepared from *S. avermitilis* after growth for 36 h (when filipin is actively produced). Primers were designed to obtain cDNAs corresponding to unabated transcription between two genes (Table S1). Transcripts were analyzed after 40 PCR cycles to ensure that even low-level transcribed genes were detected. A primer pair designed to amplify a cDNA of the *rrnA1* gene was used as an internal control. These analyses were carried out at least three times for each primer pair. Following this strategy, *pteA3*, *pteA4*, *pteA5*, *pteB*, *pteC*, *pteD* and *pteE* could be co-transcribed since unabated transcription was observed between the upstream and the downstream gene, though *pteD* has its own promoter (see below). Similarly, *pteA1* and *pteA2* and *pteF* and *pteG* could form bicistronic transcripts, though *pteA2* and *pteG* have their own promoters (see below). No transcripts were detected connecting *pteA2* and *pteA3* or *pteG* and *pteH*, thus suggesting that *pteA3* and *pteH* should have their own promoters. The genes *pteR* and *pteF* must also have their own promoters as can be deduced from their chromosomal arrangement in a divergent manner, and the same applies to *pteA1* which is arranged divergently from its upstream gene. Figure 1 shows the deduced organization of transcriptional units.

Inactivation of pteF reduces filipin production, and gene complementation restored antifungal production

In order to determine the function of pteF, we inactivated it by using the REDIRECT gene replacement technology as indicated in "Materials and methods". Double-crossover mutants

were screened by apramycin resistance. These were verified by both PCR and Southern blot analysis (Fig. S1).

The new mutant strain *S. avermitilis* ΔpteF showed delayed sporulation when compared with *S. avermitilis* wild-type when grown on solid YEME, MM or TBO media (at least 1 day later) (Fig. 2), whereas in submerged cultures, its growth was slightly higher (Fig. 3). Regardless of sporulation delay, the spore counts of both strains were similar after growth for 14 days at 30°C on the three solid media.

The fermentation broth, produced by the new mutant strain, was extracted with ethyl acetate and analyzed for the presence of filipin III (the major component of the filipin complex). HPLC assays indicated that filipin production by the mutant strain was severely reduced when compared with the parental strain. *S. avermitilis* ΔpteF produced only about 38 % of the filipin III accumulated by the wild-type strain at 48 h (51.1 μg/l) (Fig. 3). These results suggested that PteF was a positive modulator of filipin biosynthesis.

To confirm that the gene deletion was directly responsible for the impairment on filipin production, we complemented the mutant with *pteF*. A DNA fragment containing *pteF* plus its putative promoter region was inserted into the integrative vector pSETneo, giving rise to pSETneo::pteF (see "Materials and methods"). The plasmid was then transferred from *E. coli* ET12567 [pUZ8002] to *S. avermitilis* ΔpteF by conjugation. pSETneo was also introduced into *S. avermitilis* wild-type as control. Introduction of pSETneo::pteF restored filipin biosynthesis to the control levels (Fig. 3) and also its sporulation pace, thus suggesting that the mutant phenotype was due to the regulator-encoding gene knockout.

Positive heterologous complementation suggests functional conservation of PAS-LuxR regulators

Previous studies with PteF orthologous regulator PimM had shown that gene complementation of *S. natalensis* ΔpimM mutants with single copies of other PAS/LuxR counterparts restored pimaricin production, thus suggesting the functional conservation of these regulators (Santos-Aberturas et al. 2011b). To further corroborate this finding, we studied the effect of introducing one copy of *pimM* into the genome of *S. avermitilis* ΔpteF. For that purpose, we transferred the integrative plasmid pSETneo::pimM (see "Materials and methods") by conjugation from *E. coli* ET12567 [pUZ8002] to the above said strain as described (Enríquez et al. 2006). pSETneo::pteF was also introduced as a control. Interestingly, introduction of the construct restored completely the ability of *S. avermitilis* ΔpteF to produce filipins (Fig. 3).

Quantitative analysis of expression of *pte* genes in the mutant

Total RNA was prepared from *S. avermitilis* wild-type and the mutant after growth for 36 h and used as template for gene expression analysis by reverse transcription-quantitative polymerase chain reaction (RT-qPCR). The expression levels of all *pte* genes in the mutant in relation to those of the wild-type strain (assigned a relative value of 1) are shown in Fig. 4. These analyses were carried out at least three times for each primer pair.

As expected, all structural biosynthetic genes (namely *pteA1* to *pteA5*) showed reduced transcription in *S. avermitilis* ΔpteF, indicating that the promoters controlling the expression of these genes were likely targets, directly or indirectly, for regulatory

Fig. 2 The effect of *pteF* deletion on sporulation. Spores of the parental and the mutant strains were plated on YEME, TBO and MM agar followed by incubation at 30 °C for 5 or 7 days
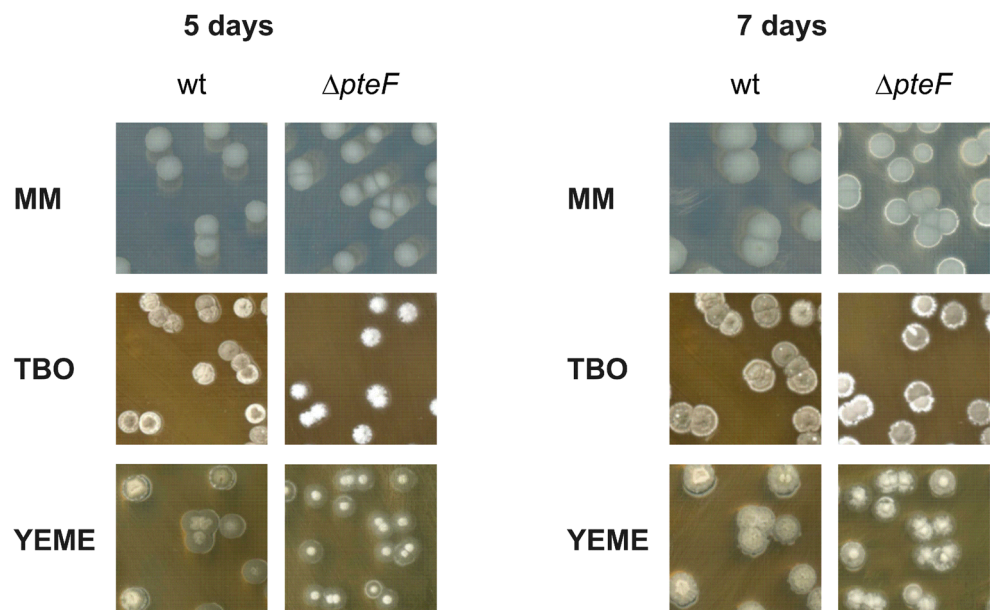
Fig. 3 Inactivation of *pteF* impairs filipin production, and gene complementation restores antifungal production. **a** *Left*: time course quantification of the filipin III production in *S. avermitilis* (*black*) and *S. avermitilis* Δ*pteF* (*grey*). *Right*: growth curves. **b** Quantification of the filipin III production attained by *S. avermitilis* Δ*pteF* complemented with *pteF* (*dark grey*) and *pimM* (*white*) genes after 48 and 72 h of growth. *S. avermitilis*::pSETneo was used as control (*black*). Data are the average of three flasks. *Vertical bars* indicate the standard deviation values. The three strains showed similar growth profiles
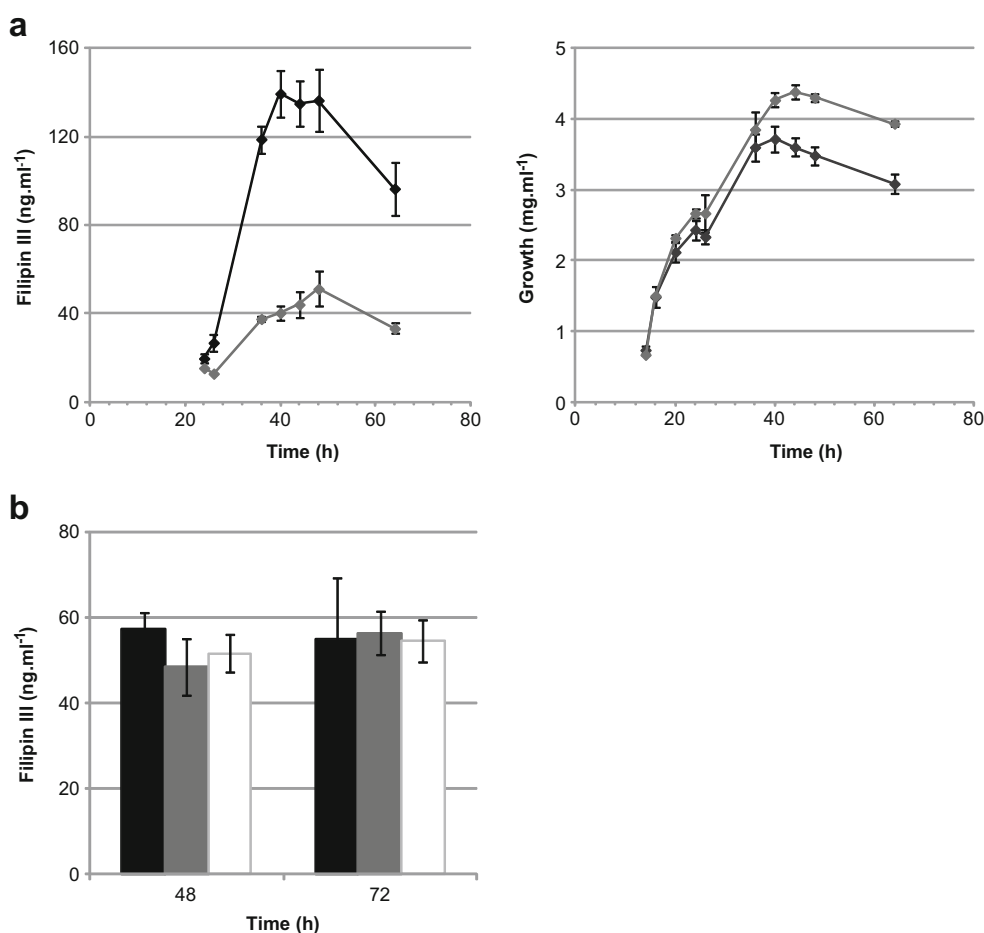
control. According to our results, these promoters were pteA1p, pteA2p and pteA3p. Control on the transcription from any of these promoters, which drive the transcription/formation of polyketide synthases in charge of building the polyketide back-bone of filipin (Ikeda et al. 2003), is sufficient to explain the reduced filipin production in the mutant. Interestingly,

Fig. 4 Gene expression analysis of the *pte* cluster in the mutant by RT-qPCR. Gene expression was assessed using RT-qPCR with the primers indicated in Table S3. The relative values are referred to 1, the assigned relative value for the expression of each gene in *S. avermitilis* NRRL 8165. The expression of *rrnA1* (encoding 16S rRNA) was used as control. Error bars were calculated by measuring the standard deviation of the ratio value among three biological and three technical replicates of each sample. The RNA templates were from 36-h cultures grown in YEME medium without sucrose. Fold change values are indicated below
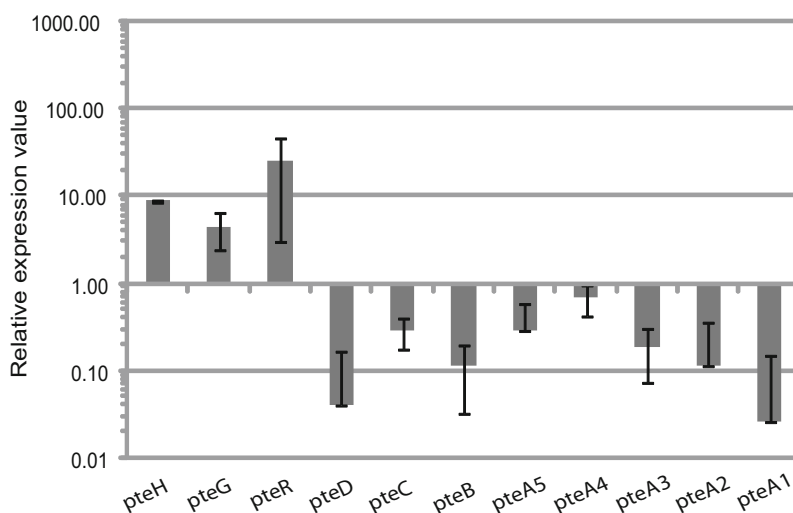
Fold change	8.7	4.4	24.6	25.0	3.6	9.1	3.6	1.5	5.6	8.3	33.3

expression values among *pteA3*, *pteA4* and *pteA5* varied considerably (Fig. 4). Given that they belong to the same operon, it is possible that the multicistronic transcript could be processed and subject to different rates of RNA degradation.

Similarly, the expression of the 2-octenoyl-CoA carboxylase/reductase encoding gene *pteB* (Yoo et al. 2011) and the cytochrome P450 encoding genes *pteC* and *pteD* (Xu et al. 2010) was also reduced. The reduced expression of *pteB* and *pteC* is in agreement with the reduced expression of *pteA3*, *pteA4* and *pteA5* given that they are thought to be co-transcribed from pteA3p. The reduced transcription of *pteD*, however, could not have been predicted since this gene has its own promoter and suggests that such promoter (pteDp) is also a target for regulatory control.

Strikingly, *pteR* expression was dramatically triggered in the mutant, showing some 25-fold more expression than in the parental strain. This clearly indicates that *pteR* promoter is a target of PteF control, although this control turned out to be indirect (see below). This result is in clear contrast to what occurs in *S. natalensis*, where *pimR* expression is not affected in *S. natalensis* Δ*pimM* mutant (Santos-Aberturas et al. 2012). Given that filipin production is reduced in the mutant when compared with the parental strain, this result could indicate that PteF either acts directly as a negative regulator on *pteR* promoter or it activates a negative regulator controlling *pteR* expression.

Interestingly, *pteG* and *pteH* expression were also triggered in the mutant. This is also in contrast with what occurs in *S. natalensis* where expression of both counterparts (*pimI* and *pimE*) is reduced in *S. natalensis* Δ*pimM* mutant.

In silico analysis of PimM targets within the *pte* cluster reveals the binding sites of PteF

Given the high degree of conservation between PteF and PimM regulators (94 % identity, Santos-Aberturas et al. 2011b), we searched for the presence of sequences similar to PimM binding site throughout the filipin cluster from *S. avermitilis*. We thus found four matching sequences, two in the intergenic region between *pteA1* and its upstream divergent gene (SAV420) and another two upstream the intergenic region between *pteA1* and *pteA2*, i.e. within *pteA1* coding sequence. According to PimM mode of action, these operators should lie in regulated promoters; thus, the first two would lie within the *pteA1* promoter region and the remaining two in the *pteA2* promoter. Table 1 shows the sequences and R_i values of the binding sites found. The sequences found in pteA1p coincide with the binding sites already identified by Santos-Aberturas et al. (2011b) and have been corroborated experimentally, whereas the sequences found in pteA2p have not been described previously. This is because according to the results presented here, *pteA2* promoter lies within the coding sequence of the upstream gene *pteA1*, and in this

position, some 180 nucleotides upstream from *pteA1* stop codon was unexpected (see below). It is noteworthy that no operator was identified in the promoter region of *pteA3*, thus suggesting that the control exerted by PteF on *pteA3A4A5BC* transcription must be indirect. Similarly, no operators were found in the promoters of *pteD*, *pteG*, *pteH* or the bidirectional promoter region *pteFR*, thus suggesting an indirect control of PteF on the expression of these genes.

PimM^{DBD} binds two targets within the filipin cluster

Incubation of GST-PimM^{DBD} with each labelled DNA fragment from the putative promoter regions selected was assessed (Fig. 5) using an electrophoretic mobility shift assay (EMSA). For each experiment, two negative control reactions were performed: absence of protein and use of GST (isolated separately). The appearance of retarded band(s) was observed upon incubation of GST-PimM^{DBD} with all the promoter regions selected, whereas it was not with the upstream regions of genes which did not contain sequences that fit the consensus. The intensity of the retarded band(s) was diminished by the addition of the same unlabeled DNA and increased when a higher concentration of protein was used (Fig. 5).

As expected, the regions retarded by GST-PimM^{DBD} were the *pteA1* promoter (two retardation bands) and the *pteA2* promoter (two shifted bands) (Fig. 5b). Upstream regions of other genes such as *pteA3*, *pteA4*, *pteR*, *pteH* or *pteG* were not retarded, indicating that PimM does not interact with them. In all cases, control reactions made with pure GST protein were negative, excluding a possible binding of this protein to the promoters. The specificity of binding of GST-PimM^{DBD} to target promoters was previously demonstrated by competition EMSA assays (Santos-Aberturas et al. 2011a).

Table 1 Regulator binding sites found in the *pte* cluster

Promoter	Strand	Sequence	R_i score
Consensus sequence		CTVGGGAWWTCCCBAG	
pteA1p (1)	−	TTAGGGGAATCCCCAA	12.19
pteA1p (1)	+	CTAGGGTTCTCCTTAG	10.77
pteA1p (2)	−	CTAAGGAGAACCCTAG	11.36
pteA1p (2)	+	TTGGGGATTCCCCTAA	12.91
pteA2p (1)	−	GTCAGGAAATCCCGAA	11.69
pteA2p (1)	+	TTCGGGATTTCCTGAC	13.23
pteA2p (2)	−	GTAGGGAATCCACTAG	10.62
pteA2p (2)	+	CTAGTGGATTCCCTAC	11.08

Information content of each binding site are indicated as R_i (Schneider 1997)

V=A, C or C; W=A or T; B=C, G or T

Fig. 5 Electrophoretic mobility analyses (EMSA). **a** Electrophoretic mobility analysis of GST-PimM binding to different promoter regions. Promoter names are indicated above the pictures. All experiments were carried out with 10-ng labelled DNA probe and 20 nM of GST-PimM^{DBD} protein. **b** *Left panel*: binding to *pteA1* and *pteA2* promoter regions with increasing concentrations of GST-PimM^{DBD}. *Central panel*: competition experiment between labelled *pteA2p* and unlabeled *pteA2p* and between *pteA2p* and *pteA3p*. Note that 150-fold-higher concentrations of *pteA3p* competitor DNA failed to decrease the intensity of the *pteA2p* retardation bands. Both experiments were performed with 11 nM of GST-PimM^{DBD} protein. *Right panel*: control reactions with 60 μM of pure GST protein. In all cases, *lane C* indicates control without protein
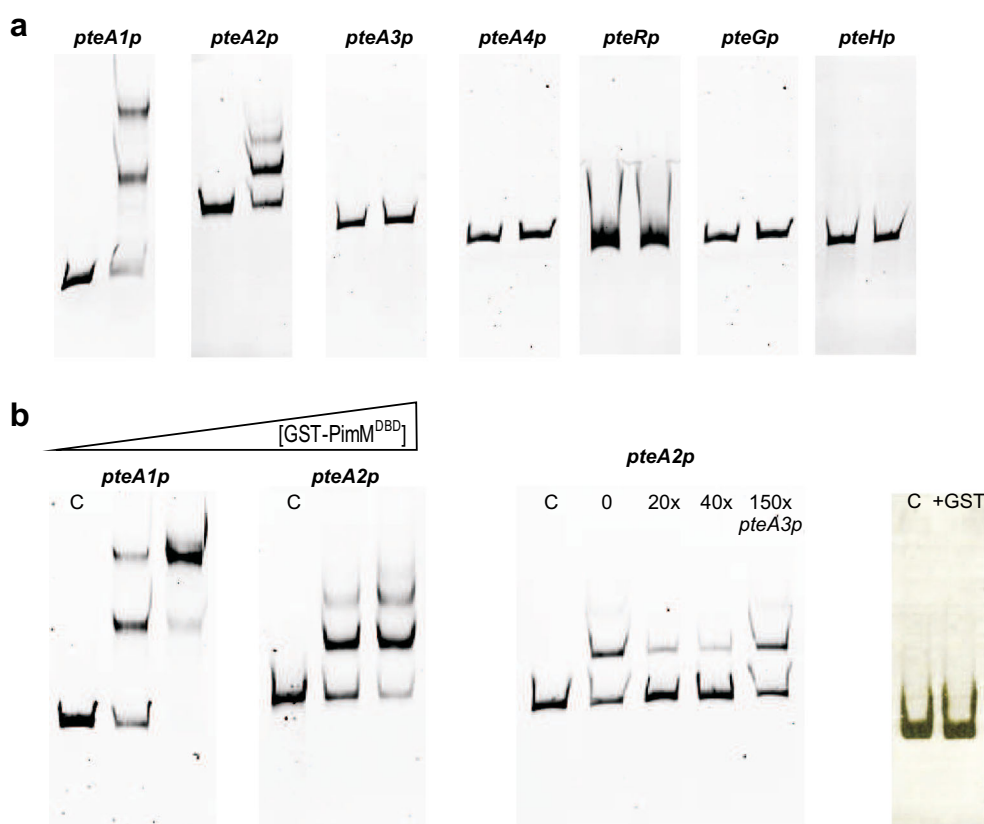
Characterization of promoters

To determine the transcriptional start sites of promoters, 5′-RACE experiments were carried out. Once the +1 sites were known, the corresponding -10 and -35 boxes of each promoter were established by comparison with the matrices reported by Bourn and Babb (1995) for *Streptomyces* that take into account the nucleotides occurring in 13-nucleotide stretches, including the -10 or -35 consensus hexamers (see "Materials and methods"). Results are summarized in Fig. 6. Only the promoters identified above gave positive results in 5′-RACE experiments.

The *pteH* transcription start point (TSP) is located at a thymine 212 bp upstream from the GTG start codon. Analysis of the region upstream of the TSP revealed that the -10 box with the highest score to the consensus *Streptomyces* was GAACCT, centred at eight nucleotides from the start site. A search using combined class C-class A matrices (Bourn and Babb 1995) revealed a -35 box ACTACG separated by 19 nucleotides, with a score of 2.02.

The TSP of *pteG* is located at a guanine 295 bp upstream from the GTG codon. Analysis of the region upstream of the TSP revealed the presence of a -10 box CAGCGC (score 1.62), centred at 12 nucleotides from the start site, and a -35 box CGCACG separated by 15 nucleotides.

A single RACE product of approximately 300 bp was observed for *pteF*. Interestingly, the TSP transcription start point corresponds to a guanine located 30 bp downstream from the currently annotated ATG start codon, i.e. internal to the *pteF* coding sequence annotated in the databases, thus proving that such annotation is incorrect (Fig. 6). The sequence GGCCTT (score 1.35), centred at position -10, constitutes the -10 consensus, and a -35 box AGGGCC (score 1.63) was identified at 18-nt distance. Given that *pteF* was wrongly annotated, we have reassigned *pteF* start codon to the next ATG methionine-encoding codon located 120 nt downstream. Noteworthy, this new start codon coincides with the one present in the *pimM* coding sequence. Thus, TSP is located 90 bp upstream the new ATG codon.

In the case of *pteR*, the TSP was located at a guanine situated 69 bp upstream from the ATG codon. The -10 and -35 boxes (CAGGAT and TTGGAA, respectively) were centred at positions -10 and -33 from the TSP and are separated by 17 nt (Fig. 6).

For *pteD*, the TSP was identified at a guanine situated 51 bp upstream from the ATG codon. The Patser analysis of the upstream sequence revealed AAACCT and CGCACG as the -10 and -35 boxes (scores 2.68 and 2.28, respectively). Both boxes are separated by 17 nt, with the -10 hexamer centred at 10 nt from the TSP.
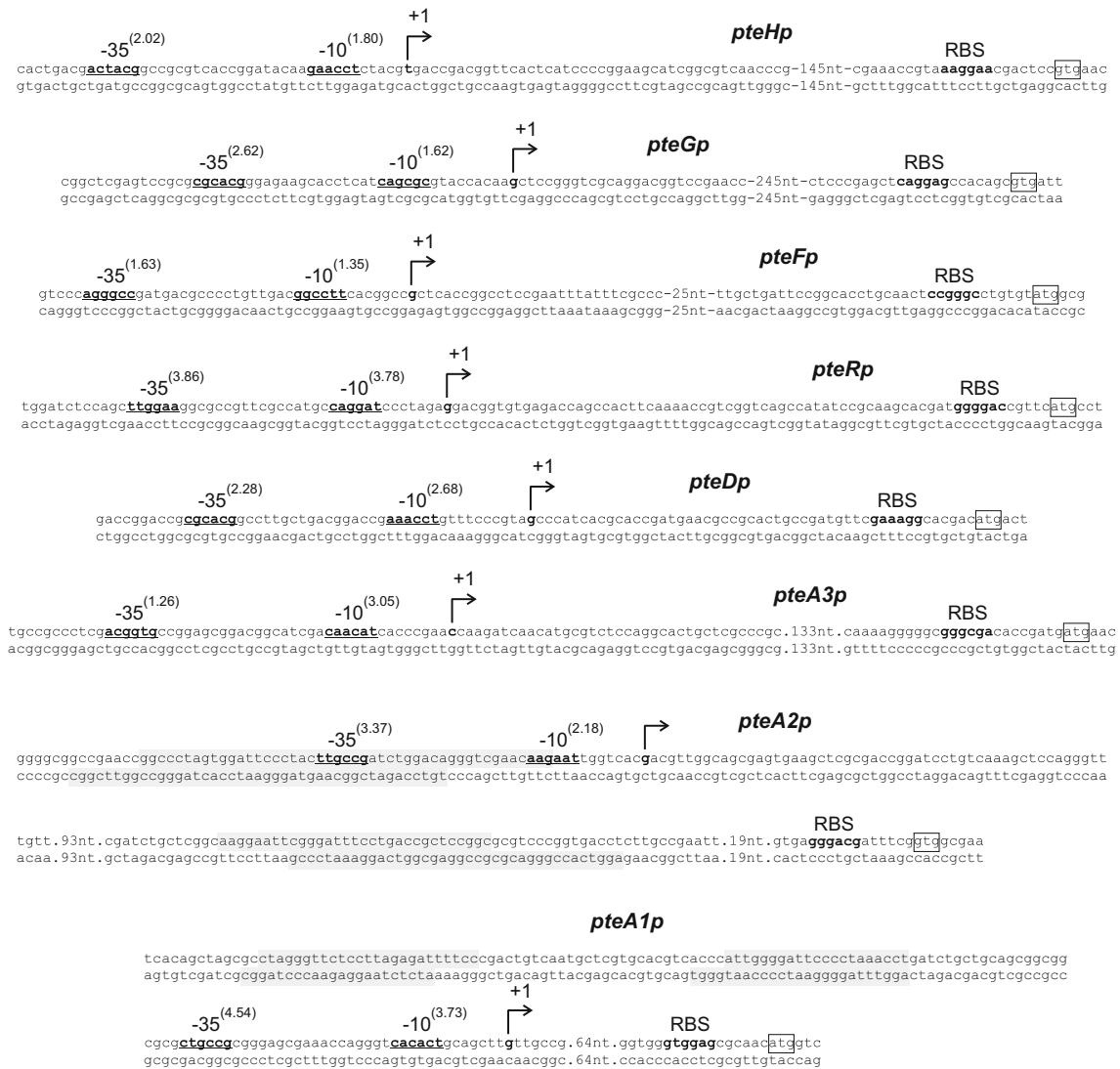
Fig. 6 Transcriptional start site of promoters. The position of the transcriptional start site was determined by 5′ RACE. The putative -10 and -35 hexanucleotides are in *bold type* and *underlined*. Scores resulting from the comparison to the matrices reported by Bourn and Babb (1995) for *Streptomyces* are indicated *between brackets*. The TSP is indicated by a *bent arrow* and *bold type letter*. Nucleotides showing homology with the 16S RNA, which could form a ribosome-binding site, are in *bold* and *labelled RBS*. The start codon is *boxed*. Protected nucleotide sequences (PteF operators) are indicated with *shaded boxes*

pteA3 TSP corresponds to a cytosine located at 196 bp from the ATG start codon, and the analysis of the sequence directly upstream revealed the presence of the -10 box as CAACAT and the -35 box as ACGGTG, with 19 nt separating them (scores 3.05 and 1.26, respectively). Noteworthy, this TSP is located 161 nt upstream from *pteA2* stop codon.

In the case of *pteA2*, a single RACE product of approximately 450 bp was observed, thus supporting the conclusion that this gene has its own promoter. The TSP of *pteA2* is located at a guanine 255 bp upstream from the GTG start codon (inside the *pteA1* coding sequence). Analysis of the region upstream of the TSP revealed the presence of a -10 box AAGAAT (score 2.18), centred at 10 nucleotides from the start site, and a -35 box TTGCCG (score 3.37) separated by 18 nucleotides (Fig. 6). Noteworthy, one of the protected regions in the coding strand lays 11 nt upstream from the TSP site, covering the -35 hexamer box of the promoter (Fig. 7).

The *pteA1* TSP is located at a guanine 88 bp upstream from the ATG codon, the -10 box CACACT is centred at 10 nt from the TSP and the -35 box CTGCCG is at an 18-nt distance (Fig. 6). Strikingly, and contrary to what occurs in *pteA2p* and in *S. natalensis*, in this case, the protected regions did not cover the -35 hexamer of the promoter and were located at 61 and 109 nt from the TSP.
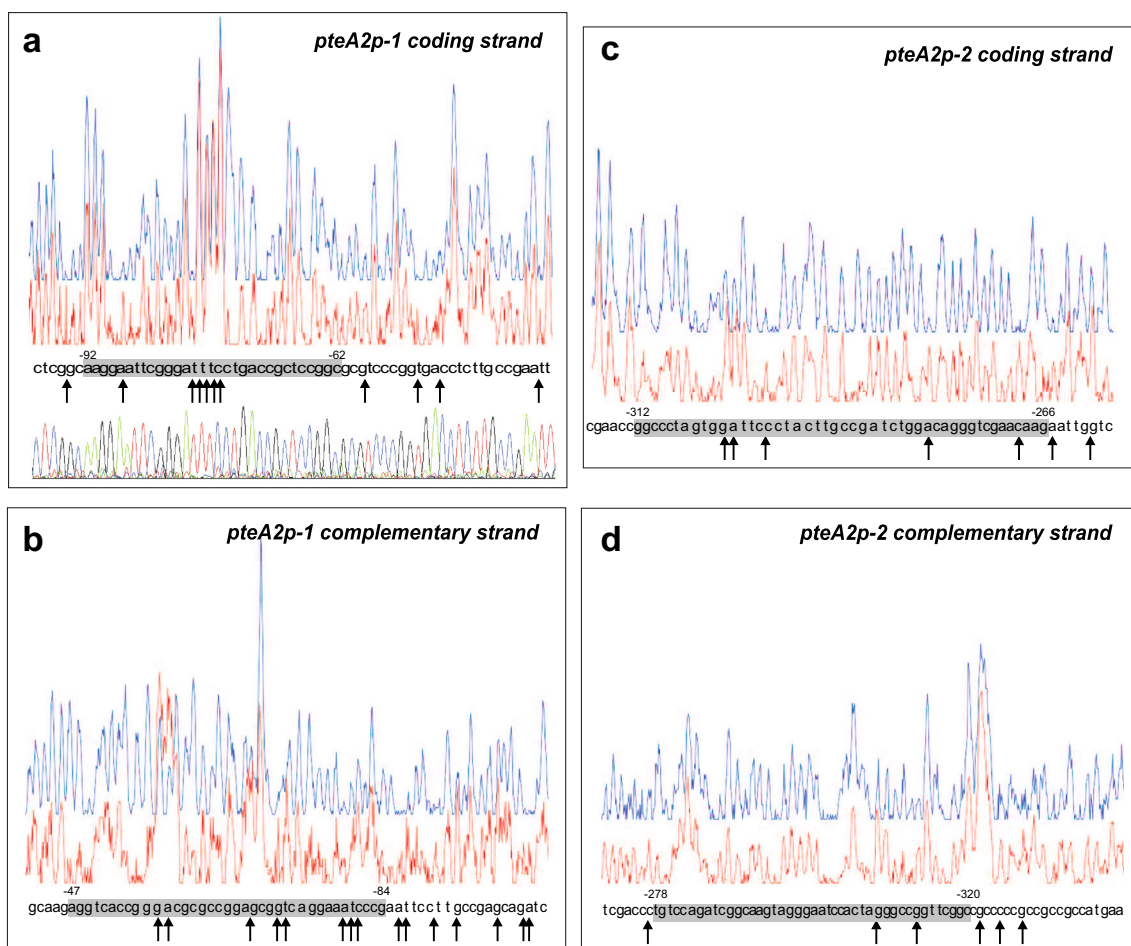
Fig. 7 **a**–**d** DNase I footprints of the GST-PimM^{DBD} protein bound to the promoter region of *pteA2*. In each panel, the upper electropherogram (*blue line*) is the control reaction. The protected nucleotide sequence is *boxed*; hyper-sensitive sites (*arrows*) are also indicated. Sequencing reactions are not included except in panel (**a**). Coordinates are from the translation start point

Dnase I protection studies reveal control over *pteA2* promoter

The promoter region of *pteA2* shown above to be retarded in EMSA was studied by DNase I protection analysis. GST-PimM^{DBD} protein (35 μM) was tested using a 5′-end fluorescein-labelled DNA fragment. Analyses were carried out in triplicate.

Results showed two major protected areas in each strand separated by some 173 nucleotides (Fig. 7), in agreement with the appearance of two retardation bands in EMSA experiments. The region closest to *pteA2* coding strand is 31-nucleotide long (positions -92 to -62 with respect to the *pteA2* translational GTG start site). The length of the protection of the reverse strand was 38 bp (positions -84 to -47), both regions being slightly displaced. The second protected area extended for 47 bp of the coding strand (positions -312 to -266 with respect to *pteA2* translational start site). The length of the protection of the reverse strand of the *pteA2* promoter was 43 bp (positions -320 to -278; Fig. 7), and both regions are displaced 8–12 nucleotides. Interestingly, DNase I

hypersensitive positions flanked the protected sequence, indicating altered DNA topology after incubation with GST-PimM^{DBD}. Some hypersensitive positions were also found inside the target sequence (Fig. 7), thus suggesting that PimM bends DNA, making those positions accessible to DNase I digestion. As expected, the protected regions contained sequences TTCGGGATTTCCTGAC and CTAGTGGATTCCCTAC that fitted well to the consensus (R_i of 13.23 and 11.08, respectively; Table 1).

Discussion

Two distinct regulators of filipin biosynthesis are encoded by genes located in the *pte* cluster, *pteR* and *pteF*. pteR belongs to a particular class of regulators that combine an N-terminal SARP domain with a C-terminal half homologous to guanylate cyclases and LAL regulators (Antón et al. 2004). Regulators of this class not only include other polyene

regulators such as the pimaricin regulator PimR (Santos-Aberturas et al. 2012) but also regulators of peptidyl nucleoside antibiotic biosynthesis such as nikkomycins (SanG) and polyoxins (PolR) (Liu et al. 2005; Li et al. 2009). In turn, PteF is a PAS/LuxR regulator. PAS/LuxR regulators combine an N-terminal PAS sensor domain with a C-terminal HTH motif of the LuxR type for DNA binding and are characteristic of polyene gene clusters (Santos-Aberturas et al. 2011b). The PAS domain detects a physical or chemical stimulus and regulates, in response, the activity of the effector domain (Möglich et al. 2009). Unlike most other sensors, proteins containing PAS domains are located in the cytosol, and therefore they detect internal signals, but they can also sense environmental factors that cross the cell membrane. The severe reduction of filipin production upon inactivation of *pteF* indicates that it behaves as an activator of filipin biosynthesis. Albeit contrary to what occurs in *S. natalensis* where inactivation of *pteF* counterpart *pimM* blocks completely polyene biosynthesis, in *S. avermitilis*, such inactivation did not halt it. This is reflected in the level of transcription of *pte* polyketide synthase genes which are still transcribed in the mutant although at a reduced rate. Notably, heterologous complementation of the mutant with the counterpart from the pimaricin gene cluster resulted in restoration of filipin production to parental levels, thus corroborating the functional conservation of these pathway-specific regulators (Santos-Aberturas et al. 2012).

Given the high degree of conservation between PteF and PimM regulators, we searched for the presence of sequences similar to the recently described PimM canonical operator (Santos-Aberturas et al. 2011b) throughout the filipin cluster from *S. avermitilis*, finding four such operators, two in the promoter region of *pteA1* (in the intergenic region between *pteA1* and its divergent gene SAV420) and another two in the upstream region of *pteA2* (both inside *pteA1* coding sequence). The presence of operators inside *pteA1* coding sequence was unexpected and suggested the location of *pteA2* promoter at that position. Interestingly, identification of the transcriptional start points by 5′-RACE corroborated the location of *pteA2* promoter at some 180 nt upstream from *pteA1* stop codon. Similarly, the TSP of *pteA3* is also located inside the upstream *pteA2* gene.

The existence of promoters inside upstream gene coding sequences is not unprecedented. Recently, Robles-Reglero et al. (2013) described the internal promoters for several *hlm* genes for holomycin production in *Streptomyces clavuligerus*. An internal promoter essential for sporulation has also been described in the *spoIIIAF* gene of *Bacillus subtilis* (Guillot and Moran 2007), and several internal promoters have been described in *Escherichia coli*, including the P2 promoter in the *trp* operon, which is located inside *trpD* (Horowitz and Platt 1982), among others.

Electrophoretic mobility shift assays were used to prove the direct binding of PimM to those regions. Two shift bands were observed upon incubation of PimM with the *pteA1* promoter, thus confirming that there were two operators in such region. Similarly, two retardation bands were observed for the *pteA2* promoter, thus suggesting that PteF controls the transcription of both genes directly. EMSAs with a different DNA probe covering pteA1p had been previously carried out with identical results (Santos-Aberturas et al. 2011b), whereas the unexpected location of *pteA2* promoter well inside the coding region of *pteA1* explains why previous attempts to perform EMSA with PimM and the intergenic region between *pteA1* and *pteA2* were unsuccessful (Santos-Aberturas et al. 2011b).

The lack of binding of PimM to the promoter regions of *pteA3*, which is thought to drive the expression of the multicistronic operon *pteA3A4A5BC*, *pteD*, which drives the expression of the bicistron *pteDE*, *pteR* or *pteG* suggests that the differential expression of these genes upon gene disruption of *pteF* is mediated by the action of another hierarchical regulator/s which would be activated by PteF. To our knowledge, there are no precedents for such conjecture, although it is conceivable given that the cross-talk between regulators has been described in the literature in several occasions (Huang et al. 2005; Santos-Beneit et al. 2009). Further experimental analyses will be required to test these hypotheses.

Footprinting analysis of pteA2p revealed two protected sequences in each strand. The protected regions in the sense strand were accompanied by protections in the complementary strand, both protected sequences being slightly displaced. This is in agreement with the binding of one monomer of GST-PimM^{DBD} to each strand of the operator. Protected sequences were flanked by DNase I hypersensitive positions, suggesting an altered DNA topology after incubation with the protein. Some hypersensitive positions were also found inside the target sequences, thus suggesting that PimM bends DNA, making those positions accessible to DNase I digestion, as it does with its natural operators in *S. natalensis* (Santos-Aberturas et al. 2011a). Identification of the transcriptional start point in the *pteA2* promoter revealed that one of the regulator binding sites overlaps with the putative -35 region, as occurs in *S. natalensis*; however, identification of the TSP in pteA1p unveiled that the two protected regions were far away from the -35 hexamer of the promoter. Although this interaction still corresponds to a class II activation mechanism, where PteF would contact domain 4 of the RNA polymerase σ subunit resulting in recruitment of RNA polymerase to the promoter, the significance of this variability is unclear (Browning and Busby 2004).

Transcription start point analysis of the *pteF* gene identified a TSP internal to the *pteF* coding sequence annotated in the databases, thus suggesting that the currently annotated sequence of *pteF* is incorrect. The coding sequence deposited in the databases starts with an ATG start codon 120 nt away

from the new ATG proposed here. Hence, this new start codon would yield a protein 40 amino acid residues shorter. This circumstance was already pinpointed by Antón et al. (2007) and is corroborated here. Besides, this TSP is preceded by conserved -10 and -35 hexamer sequences (Bourn and Babb 1995). Bearing in mind that several of the *pteF* homologues deposited in the databases are likely to have been annotated by comparison with *pteF*, based on our results, we encourage the revision of their starting codons.

Interestingly, besides being an activator of polyene production by recruiting RNA polymerase to given cluster promoters such as pteA1p or pteA2p, our results indicate that PteF must activate or repress other regulators, hence controlling indirectly the expression of other genes of the *pte* cluster. This pleiotropic behaviour is also reflected in the differential spore formation pace observed between the mutant and the parental strain. The possibility that the severe reduction on filipin production is the consequence of the delay in sporulation is unlikely given that the mutant and the wild-type strain show identical growth profiles and that the final spore titres after 14 days of growth are identical. Rather, it is conceivable that this regulator could bind operators in other sites of the chromosome, hence affecting other processes besides polyene biosynthesis, and those could be involved in sporulation. It could also be argued that filipin is required for a normal sporulation profile, but the existence of filipin nonproducing mutants not affected in sporulation precludes such possibility (unpublished).

It is interesting to note that polyene production is very low in *S. avermitilis*. Filipin III production in the wild-type strain ranged from 45 to 150 ng/ml at early stationary phase in complex media such as YEME without sucrose (Fig. 3). These values are extremely low when we compare them with the 800–1,000 μg pimaricin/ml of a standard fermentation of *S. natalensis* in the same growth medium (Recio et al. 2006). This represents some four orders of magnitude less than other polyene producers. Several factors may be the reason for such low production, the first one maybe the reduced expression of *pte* genes (unpublished), although other reasons cannot be excluded such as the high variability of fermentation yields. This variability maybe due to the described genetic instability of *S. avermitilis* (Novák et al. 1993; Chen et al. 2010), which is particularly relevant for the filipin gene cluster given its situation near one of the ends of the chromosome. Additionally, the relaxed control of PteF over its cognate promoters compared to that of PimM may also contribute to the low yields observed. Future studies will hopefully provide an answer to this question.

References

Antón N, Mendes MV, Martín JF, Aparicio JF (2004) Identification of PimR as a positive regulator of pimaricin biosynthesis in *Streptomyces natalensis*. J Bacteriol 186:2567–2575. doi:10.1128/JB.186.9.2567-2575.2004

Antón N, Santos-Aberturas J, Mendes MV, Guerra SM, Martín JF, Aparicio JF (2007) PimM, a PAS domain positive regulator of pimaricin biosynthesis in *Streptomyces natalensis*. Microbiology 53:3174–3183. doi:10.1099/mic.0.2007/009126-0

Aparicio JF, Mendes MV, Antón N, Recio E, Martín JF (2004) Polyene macrolide antibiotic biosynthesis. Curr Med Chem 11:1645–1656. doi:10.2174/0929867043365044

Bergy ME, Eble TE (1968) The filipin complex. Biochemistry 7:653–659. doi:10.1021/bi00842a021

Bi C, Rogan PK (2006) BIPAD: a web server for modeling bipartite sequence elements. BMC Bioinforma 7:76. doi:10.1186/1471-2105-7-76

Bibb MJ (2005) Regulation of secondary metabolism in Streptomycetes. Curr Opin Microbiol 8:208–215. doi:10.1016/j.mib.2005.02.016

Bourn WR, Babb B (1995) Computer assisted identification and classification of streptomycete promoters. Nucleic Acids Res 23:3696–3703. doi:10.1093/nar/23.18.3696

Browning DF, Busby SJ (2004) The regulation of bacterial transcription initiation. Nat Rev Microbiol 2:57–65. doi:10.1038/nrmicro787

Chen W, He F, Zhang X, Chen Z, Wen Y, Li J (2010) Chromosomal instability in *Streptomyces avermitilis*: major deletion in the central region and stable circularized chromosome. BMC Microbiol 10:198. doi:10.1186/1471-2180-10-198

Enríquez LL, Mendes MV, Antón N, Tunca S, Guerra SM, Martín JF, Aparicio JF (2006) An efficient gene transfer system for the pimaricin producer *Streptomyces natalensis*. FEMS Microbiol Lett 257:312–318. doi:10.1111/j.1574-6968.2006.00189.x

Gimpl G, Gehrig-Burger K (2011) Probes for studying cholesterol binding and cell biology. Steroids 76:216–231. doi:10.1016/j.steroids.2010.11.001

Guillot C, Moran CP (2007) Essential internal promoter in the *spoIIIA* locus of *Bacillus subtilis*. J Bacteriol 189:7181–7189. doi:10.1128/JB.00915-07

Gust B, Challis GL, Fowler K, Kieser T, Chater KF (2003) PCR-targeted *Streptomyces* gene replacement identifies a protein domain needed for biosynthesis of the sesquiterpene soil odor geosmin. Proc Natl Acad Sci U S A 100:1541–1546. doi:10.1073/pnas.0337542100

Hertz GZ, Stormo GD (1999) Identifying DNA and protein patterns with statistically significant alignments of multiple sequences. Bioinformatics 15:563–577. doi:10.1093/bioinformatics/15.7.563

Higgens CE, Hamill RL, Sands TH, Hoehn MM, Davis NE (1974) The occurrence of deacetoxycephalosporin C in fungi and streptomycetes. J Antibiot 27:298–300. doi:10.7164/antibiotics.27.298

Horowitz H, Platt T (1982) Identification of trp-p2, an internal promoter in the tryptophan operon of *Escherichia coli*. J Mol Biol 156:257–267. doi:10.1016/0022-2836(82)90327-8

Huang J, Shi J, Molle V, Sohlberg B, Weaver D, Bibb MJ, Karoonuthaisiri N, Lih CJ, Kao CM, Buttner MJ, Cohen SN

(2005) Cross-regulation among disparate antibiotic biosynthetic pathways of *Streptomyces coelicolor*. Mol Microbiol 58:1276–1287. doi:10.1111/j.1365-2958.2009.06624.x

Ikeda H, Ishikawa J, Hanamoto A, Shinose M, Kikuchi H, Shiba T, Sakaki Y, Hattori M, Omura S (2003) Complete genome sequence and comparative analysis of the industrial microorganism *Streptomyces avermitilis*. Nat Biotechnol 21:526–531. doi:10.1038/nbt820

Ikeda H, Shin-ya K, Omura S (2014) Genome mining of the *Streptomyces avermitilis* genome and development of genome-minimized hosts for heterologous expression of biosynthetic gene clusters. J Ind Microbiol Biotechnol 41:233–250. doi:10.1007/s10295-013-1327-x

Kieser T, Bibb MJ, Buttner MJ, Chater KF, Hopwood DA (2000) Practical *Streptomyces* genetics. John Innes Foundation, Norwich

Kim JD, Han JW, Hwang IC, Lee D, Kim BS (2012) Identification and biocontrol efficacy of *Streptomyces miharaensis* producing filipin III against *Fusarium wilt*. J Basic Microbiol 52:150–159. doi:10.1002/jobm.201100134

Kruth HS, Comlyg ME, Butlerll JD, Vanierl MT, Finks JK, Wenger DA, Patel S, Pentchev PG (1986) Type C Niemann-Pick disease: abnormal metabolism of low density lipoprotein in homozygous and heterozygous fibroblasts. J Biol Chem 261:16769–16774

Li R, Xie Z, Tian Y, Yang H, Chen W, You D, Liu G, Deng Z, Tan H (2009) *polR*, a pathway-specific transcriptional regulatory gene, positively controls polyoxin biosynthesis in *Streptomyces cacaoi* subsp. *asoensis*. Microbiology 155:1819–1831. doi:10.1099/mic.0.028639-0

Liu G, Tian Y, Yang H, Tan H (2005) A pathway-specific transcriptional regulatory gene for nikkomycin biosynthesis in *Streptomyces ansochromogenes* that also influences coloy development. Mol Microbiol 55:1855–1866. doi:10.1111/j.1365-2958.2005.04512.x

Liu G, Chater KF, Chandra G, Niu G, Tan H (2013) Molecular regulation of antibiotic biosynthesis in *Streptomyces*. Microbiol Mol Biol Rev 77:112–143. doi:10.1128/MMBR.00054-12

Martín JF, Liras P (2010) Engineering of regulatory cascades and networks controlling antibiotic biosynthesis in *Streptomyces*. Curr Opin Microbiol 13:263–273. doi:10.1016/j.mib.2010.02.008

Martín JF, Gutiérrez S, Aparicio JF (2000) Secondary metabolites. In: Lederberg J (ed) Encyclopedia of microbiology, 2nd edn. Academic, San Diego, pp 213–236, Vol. 4

Möglich A, Ayers RA, Moffat K (2009) Structure and signaling mechanism of Per-ARNT-Sim domains. Structure 17:1282–1294. doi:10.1016/j.str.2009.08.011

Novák J, Kopecký J, Kofronová O, Vaněk Z (1993) Instability of the production of avermectins, sporulation, and pigmentation in *Streptomyces avermitilis*. Can J Microbiol 39:265–267. doi:10.1139/m93-038

Omura S, Ikeda H, Ishikawa J, Hanamoto A, Takahashi C, Shinose M, Takahashi Y, Horikawa H, Nakazawa H, Osonoe T, Kikuchi H, Shiba T, Sakaki Y, Hattori M (2001) Genome sequence of an industrial microorganism *Streptomyces avermitilis*: deducing the ability of producing secondary metabolites. Proc Natl Acad Sci U S A 98:12215–12220. doi:10.1073/pnas.211433198

Pfaffl MW (2001) A new mathematical model for relative quantification in real-time RT-PCR. Nucleic Acids Res 29:e45. doi:10.1093/nar/29.9.e45

Pfaffl MW, Horgan GW, Dempfle L (2002) Relative expression software tool (REST) for group-wise comparison and statistical analysis of relative expression results in real-time PCR. Nucleic Acids Res 30:e36. doi:10.1093/nar/30.9.e36

Rasmussen R (2000) Quantification on the LightCycler. In: Meuer S, Wittwer C, Nakagawara K (eds) Rapid cycle real-time PCR, methods and applications. Springer, Heidelberg, pp 21–34

Recio E, Aparicio JF, Rumbero A, Martín JF (2006) Glycerol, ethylene glycol and propanediol elicit pimaricin biosynthesis in the PI-factor defective strain *Streptomyces natalensis npi*287 and increase polyene production in several wild type actinomycetes. Microbiology 152:3147–3156. doi:10.1099/mic.0.28953-0

Robles-Reglero V, Santamarta I, Álvarez-Álvarez R, Martin JF, Liras P (2013) Transcriptional analysis and proteomics of the holomycin gene cluster in overproducer mutants of *Streptomyces clavuligerus*. J Biotechnol 163:69–76. doi:10.1016/j.jbiotec.2012.09.017

Rozen S, Skaletsky HJ (2000) Primer3 on the WWW for general users and for biologist programmers. In: Krawetz S, Misener S (eds) Bioinformatics methods and protocols: methods in molecular biology. Humana Press, Totowa, pp 365–386

Sambrook J, Russell DW (2001) Molecular cloning: a laboratory manual, 3rd edn. N.Y. Cold Spring Harbor Laboratory Press, Cold Spring Harbor

Santos-Aberturas J, Vicente CM, Guerra SM, Payero TD, Martín JF, Aparicio JF (2011a) Molecular control of polyene macrolide biosynthesis: direct binding of the regulator PimM to eight promoters of pimaricin genes and identification of binding boxes. J Biol Chem 286:9150–9161. doi:10.1074/jbc.M110.182428

Santos-Aberturas J, Payero TD, Vicente CM, Guerra SM, Cañibano C, Martín JF, Aparicio JF (2011b) Functional conservation of PAS-LuxR transcriptional regulators in polyene macrolide biosynthesis. Metab Eng 13:756–767. doi:10.1016/j.ymben.2011.09.011

Santos-Aberturas J, Vicente CM, Payero TD, Martín-Sánchez L, Cañibano C, Martín JF, Aparicio JF (2012) Hierarchical control on polyene macrolide biosynthesis: PimR modulates pimaricin production via the PAS-LuxR transcriptional activator PimM. PLoS One 7: e38536. doi:10.1371/journal.pone.0038536

Santos-Beneit F, Rodríguez-García A, Sola-Landa A, Martín JF (2009) Cross-talk between two global regulators in Streptomyces: PhoP and AfsR interact in the control of *afsS*, *pstS* and *phoRP* transcription. Mol Microbiol 72:53–68. doi:10.1111/j.1365-2958.2009.06624.x

Schneider TD (1997) Information content of individual genetic sequences. J Theor Biol 189:427–441. doi:10.1006/jtbi.1997.0540

Schroeder A, Mueller O, Stocker S, Salowsky R, Leiber M, Gassmann M, Lightfoot S, Menzel W, Granzow M, Ragg T (2006) The RIN: an RNA integrity number for assigning integrity values to RNA measurements. BMC Mol Biol 7:3. doi:10.1186/1471-2199-7-3

van Helden J (2003) Regulatory sequence analysis tools. Nucleic Acids Res 31:3593–3596. doi:10.1093/nar/gkg567

Vicente CM, Santos-Aberturas J, Guerra SM, Payero TD, Martín JF, Aparicio JF (2009) PimT, an amino acid exporter controls polyene production via secretion of the quorum sensing pimaricin-inducer PI-factor in *Streptomyces natalensis*. Microb Cell Fact 8:33. doi:10.1186/1475-2859-8-33

Whitfield GB, Brock TD, Ammann A, Gottlieb D, Carter HE (1955) Filipin, an antifungal antibiotic: isolation and properties. J Am Chem Soc 77:4799–4801. doi:10.1021/ja01623a032

Xu LH, Fushinobu S, Takamatsu S, Wakagi T, Ikeda H, Shoun H (2010) Regio- and stereospecificity of filipin hydroxylation sites revealed by crystal structures of cytochrome P450 105P1 and 105D6 from *Streptomyces avermitilis*. J Biol Chem 285:16844–16853. doi:10.1074/jbc.M109.092460

Yoo HG, Kwon SY, Kim S, Karki S, Park ZY, Kwon HJ (2011) Characterization of 2-octenoyl-CoA carboxylase/reductase utilizing *pteB* from *Streptomyces avermitilis*. Biosci Biotechnol Biochem 75: 1191–1193. doi:10.1271/bbb.110003